PERGAMON

International Journal of Heat and Mass Transfer 44 (2001) 3919–3930

International Journal of HEAT and MASS TRANSFER

www.elsevier.com/locate/ijhmt

Transient mass and heat transfer in a smooth pipe

N. Mahinpey [a,b], M. Ojha [a,b], O. Trass [a,*]

[a] Department of Chemical Engineering, University of Toronto, Toronto, Ont., Canada M5S 3E5

[b] Institute of Biomaterials and Biomedical Engineering, University of Toronto, Toronto, Ont., Canada M5S 3E5

Received 31 March 2000; received in revised form 20 December 2000

Abstract

The electrochemical technique with the ferri-ferrocyanide system has been used to obtain transient mass transfer coefficients for smooth pipes. In contrast to the analytical solution of the corresponding heat transfer problem, two distinct transient periods are observed. It is proposed that the first is controlled by chemical reaction kinetics at the surface and during that period the boundary condition of zero ferricyanide concentration at the cathode surface is approached. The diffusion-controlled period follows in agreement with the heat transfer solution. The transfer rate for laminar flow is then proportional to $(D/t)^{1/2}$, in accordance with Higbie's penetration theory. By analogy, the data also confirm the analytical heat transfer results. In turbulent flow, the mass transfer rate during the first transient period is the same as in laminar flow; during the second, it is proportional to $Re^{1/4}(D/t)^{1/2}$, higher than in laminar flow. Therefore, the first transient period is longer and the second shorter than for laminar flow conditions.

1. Introduction

In heat or mass transfer to and from flowing systems one distinguishes between the entry region of a conduit and the fully developed region which occurs further downstream. In the former, temperature and concentration changes are confined to a thin boundary layer near the wall; in the latter, these variations penetrate into the core of the fluid.

Heat and mass transfer coefficients in the entry region are well established for steady laminar flow. They were first studied by Leveque [1] and can be cast in the dimensionless form for constant temperature or concentration boundary conditions as

$$Sh = 1.615(ReSc(d/L))^{1/3}, \quad (1)$$

$$Nu = 1.615(RePr(d/L))^{1/3}. \quad (2)$$

For the transient period which precedes attainment of the steady state, no experimental data and little theoretical work can be found in the literature, although the importance of transient, or more generally unsteady, behaviour is undeniable in many areas of transport phenomena. For example, in a pulse-plating operation, the current is turned off periodically for short intervals to allow the concentration of metal ions to increase at the electrode surface. This procedure is useful in producing an improved deposit morphology. There are many other industrial applications where a knowledge of transient behaviour is essential for the design of control systems.

The occurrence of unsteady mass transfer is also seen in biological systems and has been discussed by Basmadjian et al. [2] in the context of blood coagulation. "The First Hundred Seconds" and "The Breathing Reactor" are two important cases of unsteady physiological mass transfer. The former, which is of particular interest here, represents the changes immediately after the coagulation cascade is triggered by a reactive event at the blood/wall interface. The concentration boundary layer undergoes a rapid growth and, since the fate of the coagulation process may be determined by the wall concentration changes (transients), it would be of importance to have some insights into this interval. Furthermore, transients may give rise to

* Corresponding author. Tel.: +1-416-978-6901; fax; +1-416-978-8605.

E-mail address: trass@chem-eng.utoronto.ca (O. Trass).

0017-9310/01/$ - see front matter
PII: S0017-9310(01)00039-4

Nomenclature

A	cathode area (m^2)
C_b	bulk concentration (mol/l)
C_w	wall concentration (mol/l)
D	diffusion coefficient (m^2/s)
d	diameter (m)
F	Faraday constant
h	heat transfer coefficient (J/m^2 s K)
I	current (A)
I_{lim}	limiting cell current (A)
k	mass transfer coefficient (m/s or cm/s)
L	length of the cathode (m)
n	valence change
Pr	Prandtl number (v/α)
Q	volumetric flow rate (m^3/s)
q_w	wall heat flux (J/m^2 s)
Re	Reynolds number (Ud/v)
Sc	Schmidt number (v/D)
Sh	Sherwood number (kd/D)
t	time (s)
t^+	dimensionless variable ($tu_\infty^2/vSc^{1/3}$)
t^*	non-dimensional time (Ut/d)
U	average velocity (m/s)
u_∞	free stream fluid velocity in x-direction
v	cell voltage (V)
x	distance along the wall (m)
x^+	dimensionless variable ($x\rho u_\infty^3/v\tau_w$)

Greek letters

α	thermal diffusivity of the fluid (m^2/s)
τ_w	wall shear stress (Pa)
τ^+	dimensionless variable ($t^+/(x^+)^{2/3}$)
v	kinematic viscosity (m^2/s)
ρ	density (kg/m^3)
δ	concentration boundary layer thickness (m)

Subscript

ss	steady state

large overshoots and lag times in the next phase of the coagulation cascade called ''common pathway'' and, hence, both the steady and unsteady states need to be scrutinized [3].

In ''The Breathing Reactor'', flow pulsatility will culminate in an unsteady process. The mass transfer coefficient and the concentration boundary layer undergo periodic variations as the flow rate increases, diminishes and reverses itself during the course of a blood pulse cycle.

Soliman and Chambre [4] treated the time-dependent Leveque problem. In 1990, Basmadjian [5], in some parts of a detailed review, discussed unsteady-state mass transfer in physiological systems. These two references are of particular relevance to the present work, in which transient heat and mass transfer in the entry region of a circular pipe are examined both experimentally and theoretically.

2. Theory

As previously mentioned, the time-dependent boundary layer growth in the Leveque region has been analyzed by Soliman and Chambre [4]. They generalized the steady-state Leveque problem to include time dependence for the surface heat flux due to a time-step in the surface temperature and for the case of the surface temperature due to a time-step in the wall heat flux. Their solution for the heat flux when the Prandtl number, Pr, is very large was given in the following expanded form in powers of a dimensionless parameter τ^+:

$$\frac{q_w}{q_{w,ss}} = \frac{1.0480}{\sqrt{\tau^+}} - 0.1376 + 0.(\tau^+) + 6.9177(\tau^+)^2 + 10.029(\tau^+)^3 - 0.(\tau^+)^4, \tag{3}$$

where

$$\tau^+ = \frac{t^+}{(x^+)^{2/3}}. \tag{4}$$

As $\tau^+ \to 0$, this equation reduces to

$$\frac{q_w}{q_{w,ss}} \approx \frac{1.048}{\sqrt{\tau^+}}. \tag{5}$$

Based on the plots in [4], Eqs. (3) and (5) are identical to within 10% of $q_{w,ss}$. Now, one may use the analogy between heat and mass transfer to establish

$$\frac{N}{N_{ss}} = \frac{k(C_b - C_w)}{k_{ss}(C_b - C_w)_{ss}} \approx \frac{1.048}{\sqrt{\tau^+}}, \tag{6}$$

in which C_b and C_w are the concentrations of the reacting ion in the bulk of the solution and at the wall, respectively.

In a mass-transfer-controlled regime it follows that

$$\frac{k}{k_{ss}} \approx \frac{1.048}{\sqrt{\tau^+}} = 1.048\frac{\mu^{1/3}x^{1/3}}{t^{1/2}D^{1/6}\tau_w^{1/3}}. \tag{7}$$

To evaluate the transient mass transfer coefficients, k, in this equation, we introduce the steady state value, k_{ss}, obtained from the Leveque solution for the local position x:

$$Sh = \frac{k_{ss}d}{D} = 1.076(Re\,Sc(d/x))^{1/3} = 1.076\left(\frac{Ud^2}{Dx}\right)^{1/3}. \quad (8)$$

Inserting the wall shear stress, τ_w, from the Poiseuille solution for pipe flow

$$\tau_w = \frac{8U\mu}{d} \quad (9)$$

into Eq. (8) gives

$$Sh = 0.54\left(\frac{\tau_w}{D\mu x}\right)^{1/3} \quad (10)$$

and, hence, the steady-state mass transfer coefficients can be expressed as

$$k_{ss} = 0.54\left(\frac{\tau_w D^2}{\mu x}\right)^{1/3}. \quad (11)$$

Replacing k_{ss} in Eq. (7) finally gives

$$k = 0.57\left(\frac{D}{t}\right)^{1/2}. \quad (12)$$

This simplified version of Eq. (3) indicates that the transient mass transfer coefficients for the laminar regime are, in contrast to the steady-state values, independent of velocity and distance. Its heat transfer counterpart is

$$\frac{h}{\rho C_p} = 0.57\left(\frac{\alpha}{t}\right)^{1/2}, \quad (13)$$

where h and α are the heat transfer coefficient and thermal diffusivity, respectively.

It should be noted that the transient mass transfer coefficient k in Eq. (12) is identical to that derived by Higbie [6] in his "penetration theory" for mass transfer from bubbles rising through a stagnant liquid [7],

$$k = \left(\frac{D}{\pi t}\right)^{1/2} = 0.57\left(\frac{D}{t}\right)^{1/2}. \quad (14)$$

The reason is that both of these otherwise dissimilar processes are transient and diffusion controlled.

An expression for film thickness under transient conditions can be derived directly from Eq. (12):

$$\delta \approx \frac{D}{k} = 1.75(Dt)^{1/2}. \quad (15)$$

Until local steady state is reached, δ depends on diffusivity and time only, and is independent of both velocity and position.

The transient solution can be equated with the integrated Leveque solution over the length L to obtain the time required to reach steady state.

$$0.57\left(\frac{D}{t}\right)^{1/2} = 1.615\left(\frac{UD^2}{dL}\right)^{1/3}, \quad (16)$$

where the right-hand side represents the mean integral mass transfer coefficient over the conduit length L. Solving Eq. (16) for time t, we obtain

$$t_{ss} = 0.124\left(\frac{d^2L^2}{U^2D}\right)^{1/3}. \quad (17)$$

However, since the transient solution is only valid to within 10% of the steady state and the approach is subsequently slower and more asymptotic, Eq. (17) will slightly underestimate the time required to reach steady state.

It should be noted that the transient period depends on length L. This reinforces the fact that the thin concentration or temperature boundary layers near the entrance region are built up rapidly, with the later, thicker ones taking a longer time to reach the steady-state concentration or temperature profiles.

3. Experimental

3.1. The electrochemical technique

The electrochemical technique was used to measure mass transfer coefficients between nickel surfaces and the ferri-ferrocyanide solution. This method is based on a diffusion-controlled reaction at the electrode surface. As discussed in detail by Selman and Tobias [8], when an electric potential is applied between two electrodes in an aqueous solution of an electrolyte, an ionic reduction occurs at the cathode and an oxidation at the anode. As a result, a current, which is proportional to the number of ions reacting at the electrodes per unit time, flows through the circuit.

At steady state, ions that are converted at the electrode have to be supplied from the bulk of the liquid. This can occur by a diffusion process under the influence of the concentration gradient and by migration of the ions in the electric field. The rate of the electrochemical reaction increases with the potential difference between the electrode and solution, and at a sufficiently high potential difference, mass transfer towards the electrodes becomes the rate-determining step in the electrochemical reaction. By using an extra-large anode, the flux of reacting ions is influenced primarily by the cathode geometry. In this study, the following reaction occurs at the cathode:

$$Fe(CN)_6^{3-} + e^- \rightarrow Fe(CN)_6^{4-} \quad (18)$$

and the reverse reaction at the anode. Thus, the composition of the electrolyte solution does not change.

As discussed earlier, ions may migrate due to the potential gradient. To suppress this effect or make it

negligible compared to diffusion and convection, a high concentration of sodium hydroxide (inert electrolyte) is used. This also enables the Schmidt number to be adjusted since diffusivity and viscosity of the solution depend on both temperature and NaOH concentration.

If the bulk concentration of the reacting species, C_b, is known, an average mass transfer coefficient k can be calculated from

$$k = I_{lim}/nFAC_b, \tag{19}$$

where I_{lim} is the measured limiting current, n is valency change in the reaction, F is Faraday's constant and A is the surface area of the cathode.

3.1.1. Flow loop and experimental procedure

The experimental set-up shown in Fig. 1 formed a closed loop from the 3 HP centrifugal pump through PVC pipe with an internal diameter of 38 mm, to the nickel test section, two rotameters and a 200 l polyethylene tank. An inverter was used to adjust the RPM of the pump motor and, hence, to control the flow rate. In addition to the inverter, a bypass loop was employed to control the flow rate. A 3.5 m long PVC pipe before the cathode was used to ensure fully developed flow conditions at all Reynolds numbers. The temperature of the solution was controlled by a coil heat exchanger inserted in the tank.

The solution was deoxygenated before each run by nitrogen bubbles. The concentrations of potassium ferricyanide and sodium hydroxide were checked by volumetric analysis [9] prior to each run. To obtain Schmidt numbers of 4200 and 2650, the runs were carried out at temperatures of 18°C and 28°C, respectively. The concentrations of $K_3Fe(CN)_6$, $K_4Fe(CN)_6$ and NaOH were 4×10^{-3}, 6×10^{-2} and 2.5 M, respectively. All physical properties, together with Schmidt numbers, were calculated based on data provided by Bourne et al. [10].

3.2. Electrical circuit

An 8-channel, 12-bit, analog input DAS08 board was used to measure the voltage across the electrodes as well as the current in the cell. A 0.05 Ω current shunt was placed in series with the cell in order to measure the cell current. The voltage and current signals were isolated by using two separate signal conditioning modules. The electrode voltage signal was input to a −5 to 5 V analog input/output module, which relayed an isolated signal to the DAS08 board. On the other hand, the cell current signal was input to a −100 to 100 mV analog input, −5 to 5 V analog output, which relayed an amplified isolated signal to the DAS08 board. The voltage and current data were sampled at 10 Hz for transient response experiments, and at 1/30 Hz for obtaining polarization curves. An overall schematic diagram of the electrical circuit is given in Fig. 2.

As there was a lag time between the time the data acquisition system started and the time the power supply was switched on, the first non-zero, positive current was assigned to 0.1 s, the smallest time reading, to synchronize data obtained from all runs.

3.2.1. Measurement errors

An evaluation of all sources of error has been made in [11]. The pertinent maximum uncertainties are, in the

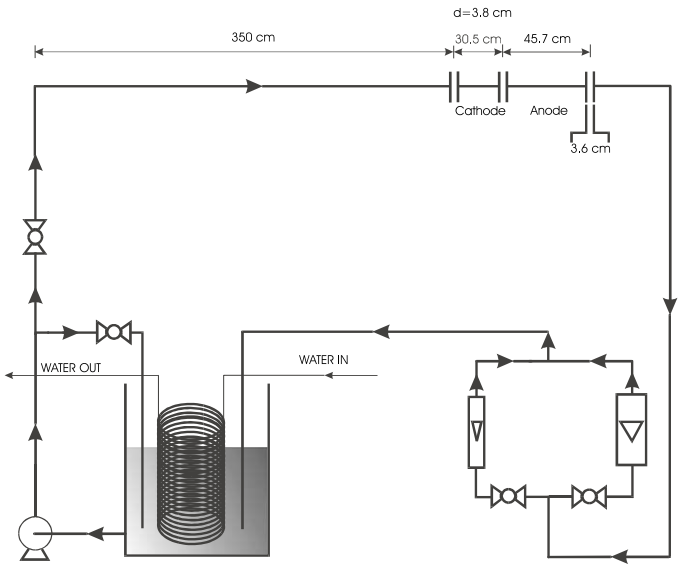

Fig. 1. Schematic diagram of electrolyte flow system.

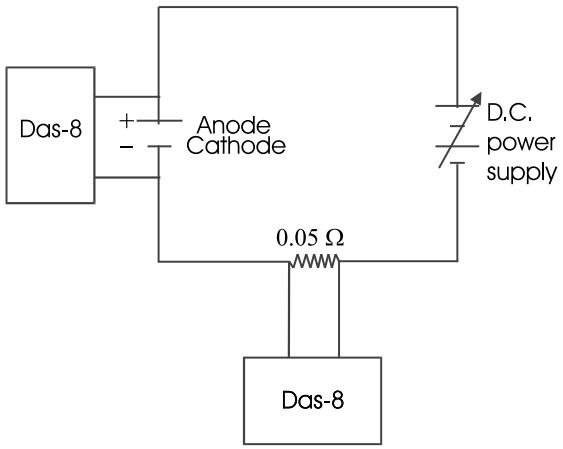

Fig. 2. Electrical circuit.

Reynolds number 3.1%, in the Schmidt number 4.1% and in the Sherwood number 4.3%.

4. Results and discussion

4.1. Initial experiments

Two sets of experiments have been carried out. The main objective of the first set was to obtain steady-state values of mass transfer coefficients in a smooth, straight pipe, 18.6 mm in diameter and 150 mm in length, and a Y-bifurcation model resembling a human aortic bifurcation [12].

Results of that earlier work revealed two distinct regions during the transient period as shown in Fig. 3, where the mass transfer coefficient k is plotted versus time. The first region with a lower slope is followed by a second one which then gradually approaches the steady-state values. The point(s) at which the slope change(s) will hereafter be called the hump. Similar results were obtained at four different Schmidt numbers for both laminar and turbulent flows. All results can be found in [11].

Soliman and Chambre [4] analyzed the corresponding transient heat transfer case. As expected, a general monotonic reduction of the transfer rate is predicted with no hump and no inflection point, as was clearly observed for electrochemical mass transfer in Fig. 3. Since heat and mass transfer are substantially governed by the same mechanism, a difference in the boundary conditions may justify this discrepancy. Soliman et al. imposed their boundary conditions at time $t = 0$. However, in our mass transfer experiments, while the cell voltage was imposed at $t = 0$, the corresponding wall boundary condition of zero ferricyanide concentration would be established only after a finite, albeit brief, period during which the reaction at the cathode is the rate-determining step. Towards the end of this period, i.e. when the wall concentration approaches zero, the slope of the experimental k vs t plot increases and approaches or coincides with the theoretical solution for diffusion-controlled conditions. It should be noted that, as a prerequisite for the electrochemical technique, the rate of reaction must be higher than the rate of mass transfer to enable the cathode surface to consume all

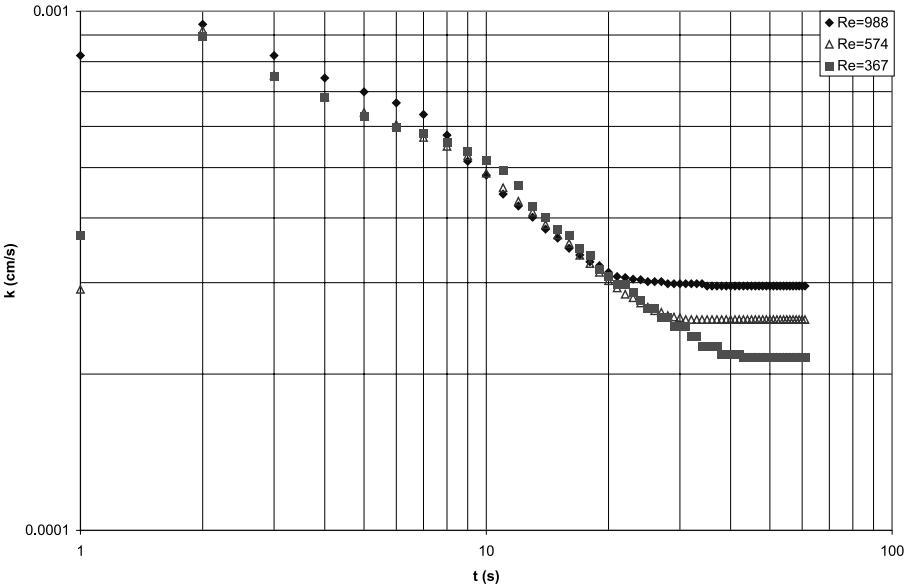

Fig. 3. Mass transfer coefficients vs time at different Reynolds numbers, $Sc = 2470$ (earlier work).

ferricyanide ions immediately upon reaching the surface. This should provide a wall concentration equal to zero, for voltages anywhere on the plateau of the polarization curve.

To test the above-mentioned hypothesis, a new set of experiments with a higher frequency of data collection was carried out. A cathode, 38 mm in diameter and 305 mm in length, and a larger anode were used. Details regarding the electrodes and their fabrication methods are given elsewhere [13].

4.1.1. Laminar flow results

In these experiments, the polarization curve was checked at each Reynolds number and the voltage across the electrodes as well as the current were recorded simultaneously with a frequency of 10 Hz, 10 times higher than previously used. Based on each polarization curve, different voltages along the plateau were applied and the currents recorded. The graphs of cell voltage vs time showed that the voltage across the cathode and anode reaches the final value in less than 1/10 of a second, for all experiments. Consequently, cell voltage lag time is not a cause of the hump.

For laminar flow, examples of mass transfer coefficients at different Reynolds and Schmidt numbers are shown in Figs. 4–6. In these figures, the line of transient behaviour obtained from the theory, Eq. (12), and the steady-state Leveque solution [1] are depicted. The time when the hump is observed and that required to reach steady state, from Eq. (17), are also shown. In the initial, reaction-rate-controlled region, since the concentration at the wall is not zero, the curves represent the ratio $k(C_b - C_w)/C_b$ rather than k; thus, the values are always lower than the transient theory line. However, after the hump, when the concentration at the wall reaches zero, the current becomes the limiting current and the ordinate correctly represents the mass transfer coefficients.

It was observed that the first transient values were higher at higher applied voltages. Also, the development of the hump was delayed as the voltage across the electrodes decreased, consistent with the decreased values of $k(C_b - C_w)/C_b$; in other words, the length of time during which the surface reaction rate governs the process becomes longer as the rate is decreased. The dependence of the level of the first transient and the resultant location of the hump on voltage reflects the dependence of the rate of the surface reaction on cell voltage.

Based on these observations, the following is proposed. When the voltage is applied to the electrodes, a mass transfer process is initiated with the formation of the concentration boundary layer. Recalling Eq. (15), one would expect, for laminar flow during the transient period, the boundary layer thickness to grow at a rate of $t^{1/2}$, independent of velocity and distance x along the cathode. Since this layer is initially very thin, the rate of mass transfer would be very high and the electrochemical process will be reaction rate limited. The initial

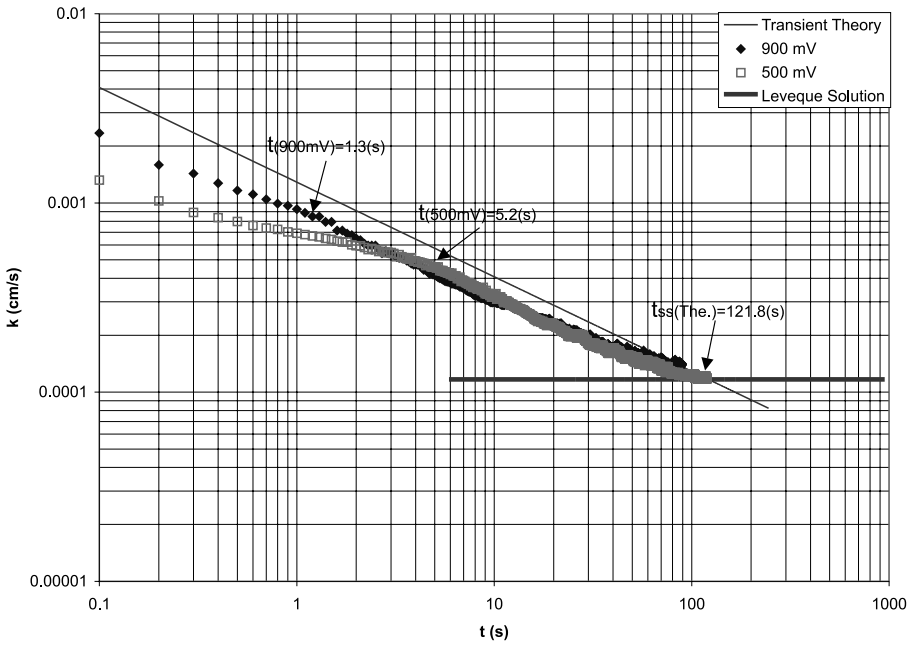

Fig. 4. Mass transfer coefficients vs time at different applied cell voltages, compared with the Leveque solution and the theoretical transient line ($Re = 473$, $Sc = 2650$).

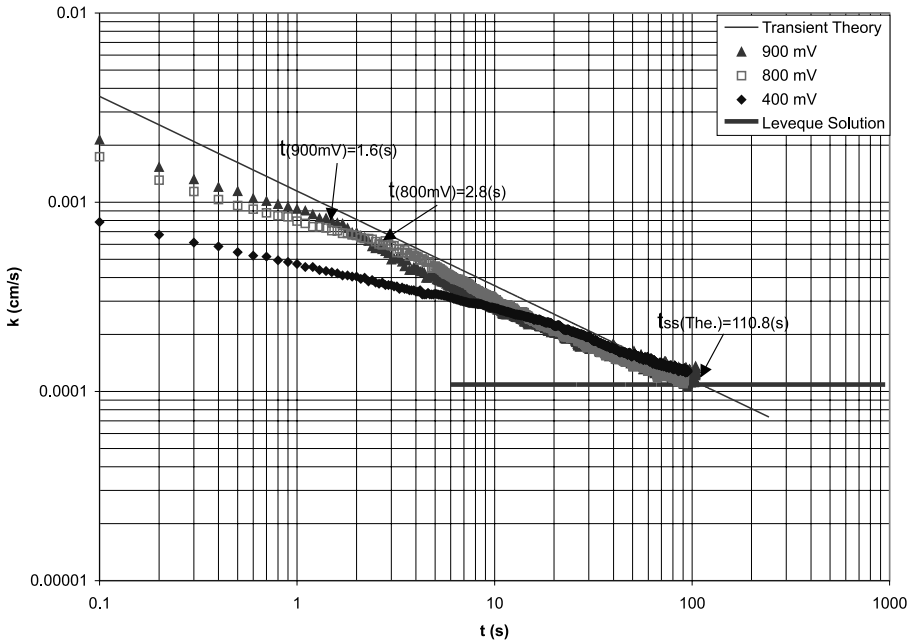

Fig. 5. Mass transfer coefficients vs time at different applied cell voltages, compared with the Leveque solution and the theoretical transient line ($Re = 488,\ Sc = 4200$).

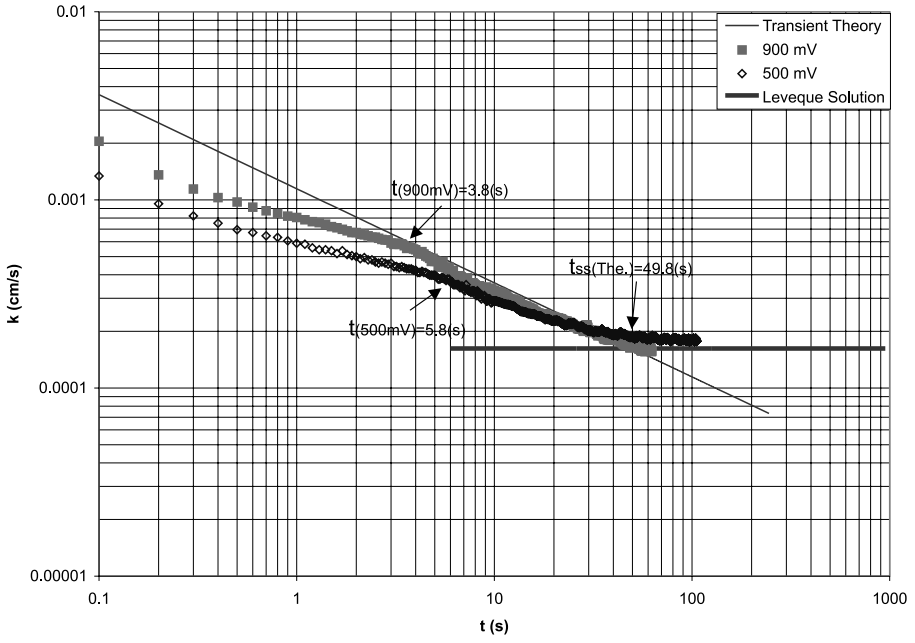

Fig. 6. Mass transfer coefficients vs time at different applied cell voltages, compared with the Leveque solution and the theoretical transient line ($Re = 1616,\ Sc = 4200$).

ferricyanide concentration at the cathode surface is the same as in the bulk (C_b). It then falls rapidly but remains above zero at the cathode surface until the hump. Thus, the initial measured current (before the hump) is largely proportional to the rate of the reaction consuming the ferricyanide ions. It is not constant but decreases slowly

due to the diminishing wall concentration. The slope of the line represents the rate of change of the reaction rate with respect to time.

Simultaneously, the concentration boundary layer grows and increases the resistance to diffusion of ferricyanide ions towards the cathode surface. This results in a decrease in the rate of mass transfer, even though $(C_b - C_w)$ increases. These two phenomena continue until the two rates are equalized and the surface concentration drops to zero. From this point on, the rate of reaction is higher than the rate of mass transfer and the process is mass-transfer-controlled. After the hump, transient mass transfer is observed until the curve approaches the steady state solution. In the second transient region, mass transfer behaviour matches that for heat transfer with a constant wall temperature.

As shown in Figs. 4–6, as the voltage across the electrodes is increased, the rate of reaction increases as well, with the k/v value at any one time remaining substantially constant, suggesting that the reaction rate varies linearly with cell voltage over the polarization plateau. Hence, the line for the reaction-rate-controlled data at higher voltages intersects earlier with the line for the mass-transfer-controlled transient data resulting in the earlier observation of the hump.

A dimensional analysis was also performed to obtain empirical transient equations. Three non-dimensional groups were introduced: Re, Sc and t^*, the latter representing non-dimensional time and given by

$$t^* = \frac{Ut}{d}. \tag{20}$$

The results are correlated with a standard deviation of 3%. In the laminar regime,

$$Sh = 0.46 Re^{0.52} Sc^{0.47} t^{*-0.48}, \tag{21}$$

$$k = Sh\frac{D}{d} = 0.46\frac{U^{0.04}}{v^{0.05}}\frac{D^{0.53}}{t^{0.48}} \propto \left(\frac{D}{t}\right)^{1/2}, \tag{22}$$

for all points from the hump to the point(s) at which deviation towards steady-state values is observed.

It is apparent that k is almost proportional to $(D/t)^{1/2}$ and that the impact of velocity or Reynolds number on k is negligible. Diffusivity and time are the main factors influencing transient mass transfer coefficients in the laminar regime, just as predicted by Eq. (12).

4.2. Turbulent flow results

Two examples of data obtained for turbulent flow are shown in Figs. 7 and 8. The same phenomena are observed as in laminar flow, with the main difference being that, for the same cell voltage, the hump occurs later. The reaction-kinetics-controlled (first transient) values are comparable to those observed in laminar flow. Once diffusional transfer is dominant, the rates for both transient and steady state are, as expected, higher than their counterparts in laminar flow. Thus, it will take

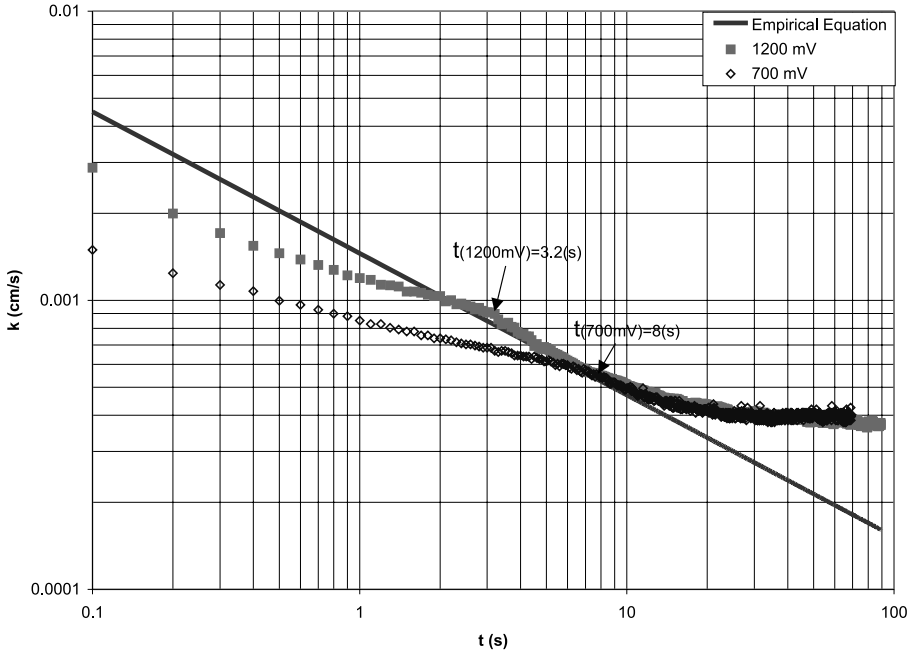

Fig. 7. Mass transfer coefficients vs time (turbulent regime), compared with the empirical correlation ($Re = 4396$, $Sc = 4200$).

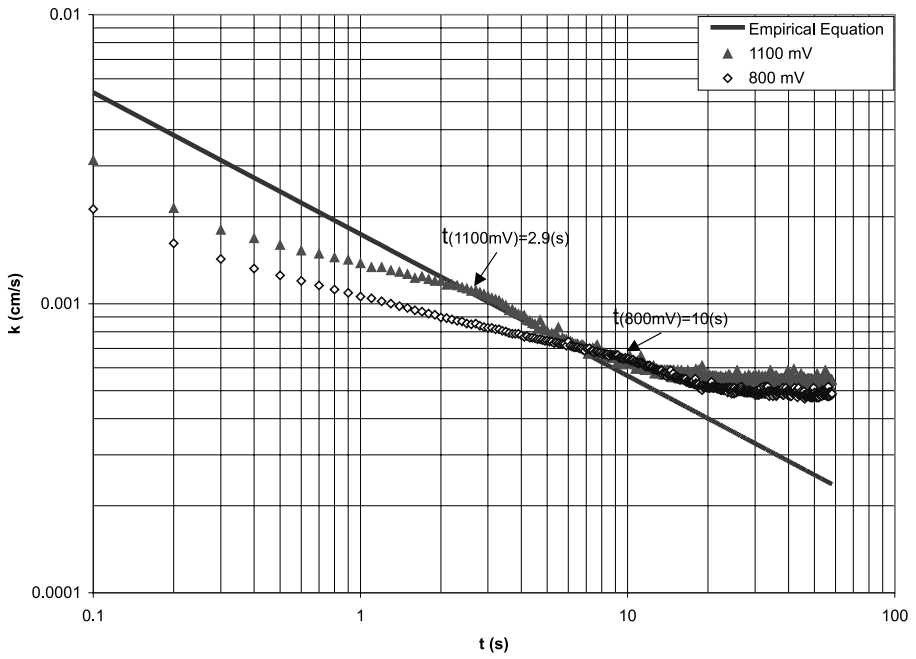

Fig. 8. Mass transfer coefficients vs time (turbulent regime), compared with the empirical correlation ($Re = 5842,\ Sc = 2650$).

longer for kinetics to catch up with the higher rate of diffusional transfer and the humps occur later. While the first transient period is longer, the second transient, the interval consistent with heat transfer results, is much shorter, i.e. the steady state condition is reached earlier. For laminar flow, this interval is 50–100 s or longer; for turbulent flow, it is 20–30 s, with shorter values for higher Reynolds and lower Schmidt numbers. The latter conditions give higher steady-state k values which are reached earlier by the transient.

The experimental results up to a Reynolds number of 7000 were correlated with a standard deviation of 3% by the expression

$$Sh = 0.09Re^{0.74}Sc^{0.51}t^{*^{-0.49}}, \tag{23}$$

$$k = Sh\frac{D}{d} = 0.09\frac{U^{0.25}d^{0.23}}{\nu^{0.23}}\frac{D^{0.49}}{t^{0.49}} \propto Re^{1/4}\left(\frac{D}{t}\right)^{1/2}. \tag{24}$$

As in the laminar case, the range of data included in the correlation is from the hump to the point at which deviation towards steady-state values is observed. Eq. (24) is also shown in Figs. 7 and 8.

Unlike laminar transient mass transfer, the Reynolds number (or velocity) does play an important role in turbulent transient mass transfer. It is also apparent that, as for laminar transient conditions, the mass transfer coefficient k depends on $(D/t)^{1/2}$. Additional turbulent data are given in Fig. 9 ($Sc = 4200$) and Fig. 10 ($Sc = 2650$) for different Reynolds numbers. All have been used for the correlation, Eq. (23). Both confirm the previous observations, viz. the long first, kinetically controlled transient, the short diffusion-controlled transient, a modest Re effect on the second transient and the stronger Re effect observed previously [12,13] for the steady-state data.

Fig. 11 shows the observed k values, i.e. $k(C_b - C_w)/C_b$, versus cell voltage at $t = 0.3$ s as an example in the first transient period for all data obtained at $Sc = 4200$. Apparently the kinetically controlled transient is substantially unaffected by flow conditions, or by the rate of diffusional transfer, and depends mainly on cell voltage. The small upward bias of the turbulent data simply suggests that turbulent eddy motion more readily replenishes the ferricyanide ion concentration at the wall, thus maintaining the C_w value slightly higher than under laminar flow conditions.

5. Summary and conclusions

Transient mass transfer coefficients have been measured in smooth pipes using the electrochemical technique. Two distinct transient regions were observed in all experiments, different from the single transient corresponding to heat transfer. In the first transient region, the process is controlled by the surface reaction rate. During this time the wall concentration of the reactant drops to zero and the boundary layer for diffusion-controlled mass transfer is established. In the second region, diffusion of the reacting ions through the boundary layer governs the process. In the first region,

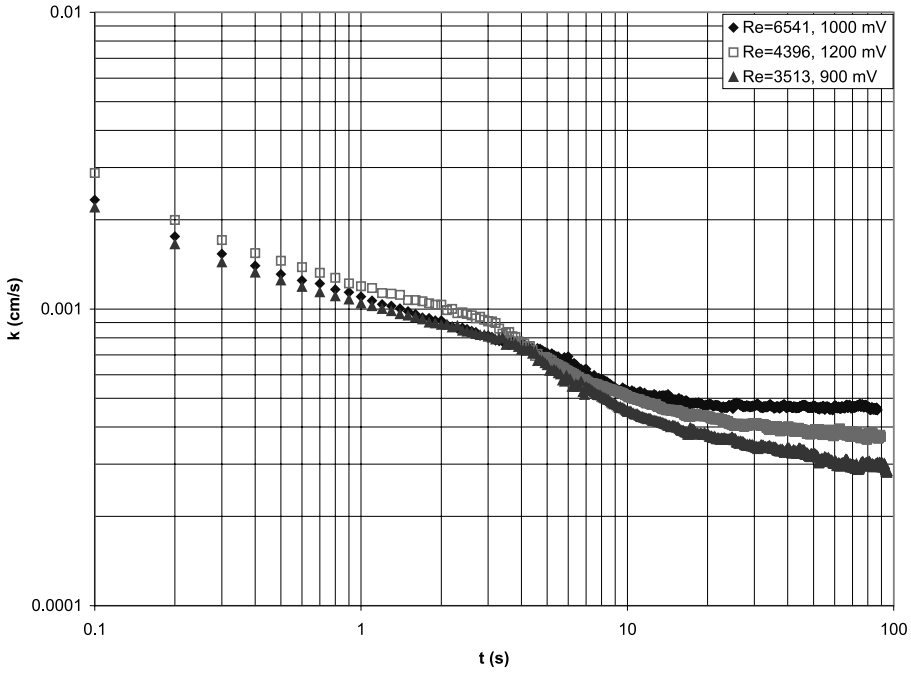

Fig. 9. Mass transfer coefficients vs time at different Reynolds numbers (turbulent regime), $Sc = 4200$.

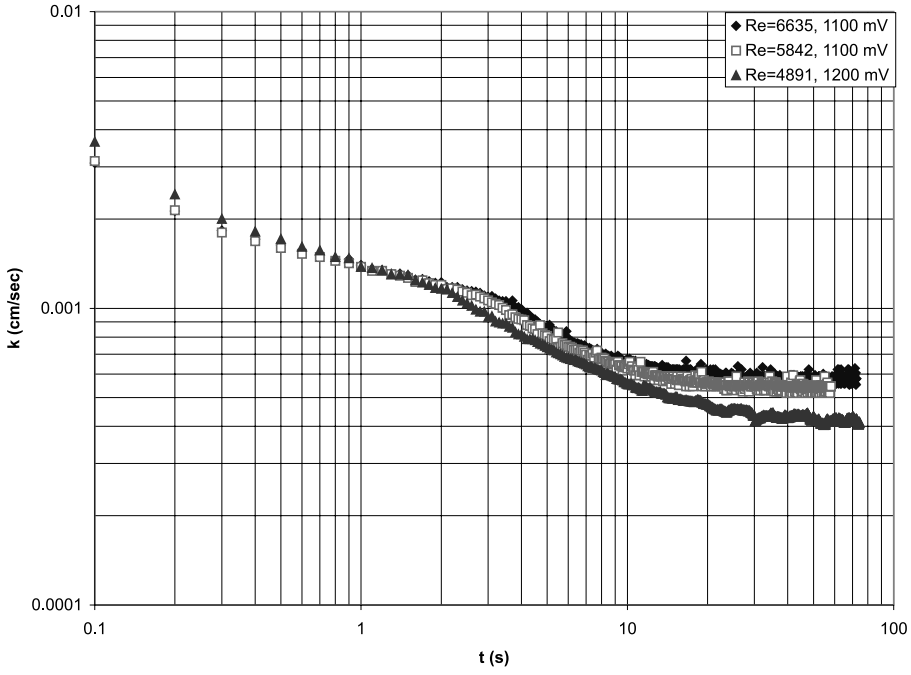

Fig. 10. Mass transfer coefficients vs time at different Reynolds numbers (turbulent regime), $Sc = 2650$.

the rate of change of the mass transfer coefficient with time is slow; as the rate speeds up in the second region, a ''hump'' is observed where the slope changes.

Support for this hypothesis was gained from measurements of reaction rate versus cell voltage (on the polarization curve plateau). A linear relationship was

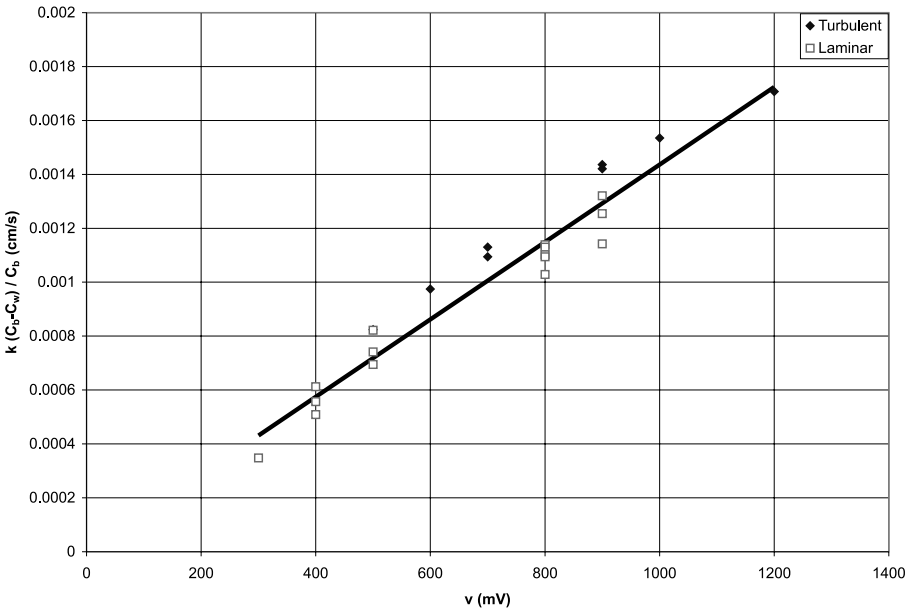

Fig. 11. Mass transfer coefficient values at $t = 0.3$ s vs applied cell voltage; laminar and turbulent results, $Sc = 4200$.

observed. The location of the hump, at which control is changed, moved toward later times as cell voltage was decreased.

In the mass-transfer-controlled transient region, the transfer rate is proportional to $(D/t)^{1/2}$, in accordance with the Higbie penetration theory and independent of velocity and distance. By analogy, the data also confirm the heat transfer results.

The same phenomena were observed in transient turbulent flow. While the kinetically controlled transient is comparable to its laminar counterpart, the transfer rate during the diffusion-controlled transient is higher than that in laminar flow. This results from the influence of velocity or Reynolds number on the transfer rate, which varies with $Re^{1/4}(D/t)^{1/2}$. Those observations and the higher steady-state transfer in turbulent flow result in a longer kinetics-controlled first transient and a shorter mass-transfer-controlled second transient period compared to those in laminar flow.

Acknowledgements

Financial assistance from the Natural Sciences and Engineering Research Council is gratefully acknowledged. The authors wish to thank Prof. D. Basmadjian for his helpful suggestions and N. Gehani for his assistance in performing the experiments. INCO Ltd. has generously supplied the nickel used to make all transfer surfaces.

References

[1] M.A. Leveque, Les lois de la transmission de chaleur par convection, Ann. Mines Mem. Ser. 13 (12) (1928) 201–415.
[2] D. Basmadjian, M.V. Sefton, S.A. Baldwin, Coagulation on biomaterials in flowing blood: some theoretical considerations, Biomaterial 18 (1997) 1511–1522.
[3] S.A. Baldwin, D. Basmadjian, A mathematical model of thrombin production in blood coagulation. Part 1. The sparsely covered membrane case, Ann. Biomed. Eng. 22 (1994) 357–370.
[4] M. Soliman, P.L. Chambre, On the time-dependent Leveque problem, Int. J. Heat Mass Transfer 10 (1967) 169–180.
[5] D. Basmadjian, The effect of flow and mass transfer in thrombogenesis, Ann. Biomed. Eng. 18 (1990) 685–709.
[6] R. Higbie, The rate of absorption of a pure gas into a still liquid during short periods of exposure, Trans. A.I.Ch.E. 31 (1935) 365–389.
[7] R.B. Bird, W.E. Stewart, E.N. Lightfoot, Transport Phenomena, Wiley, New York, 1960, p. 671.
[8] J.R. Selman, C.W. Tobias, Mass-transfer measurements by the limiting-current technique, Adv. Chem. Eng. 10 (1978) 211–318.
[9] I.M. Kolthoff, R. Belcher, Volumetric Analysis III, Interscience, New York, 1957.
[10] J.R. Bourne, P. Dell'Ava, O. Dossenbach, T. Post, Densities, viscosities, and diffusivities in aqueous sodium hydroxide–potassium ferri- and ferrocyanide solutions, J. Chem. Eng. Data 30 (1985) 160–163.
[11] N. Mahinpey, An electrochemical investigation of mass transfer in a pipe and a simplified bifurcation model, Ph.D. Thesis, University of Toronto, 2000.

[12] N. Mahinpey, M. Ojha, K.W. Johnston, O. Trass, Electrochemical mass transfer measurements in a Y bifurcation model, Can. J. Chem. Eng. 78 (2000) 902–907.

[13] W. Zhao, O. Trass, Electrochemical mass transfer measurements in rough surface pipe flow: geometrically similar V-shaped grooves, Int. J. Heat Mass Transfer 40 (1997) 2785–2797.